ELSEVIER

Polymer 41 (2000) 385–390

polymer

Modified polyacrylonitrile blends with cellulose acetate: blend properties

Byung Kyu Kim[a,*], Young Se Oh[b], Young Min Lee[a], Lee Keun Yoon[a], Soo Lee[c]

[a]*Department of Polymer Science and Engineering, Pusan National University, Pusan 609-735, South Korea*
[b]*Research and Development Center, Hanil Synthetic Fiber Company Ltd., Masan 630-791, South Korea*
[c]*Department of Chemistry, Changwon National University, Changwon 641-773, South Korea*

Received 17 September 1998; received in revised form 8 February 1999; accepted 11 February 1999

Abstract

Polyacrylonitrile (PAN) was modified by copolymerizing with methyl acrylate (MA) and 2-acrylamido-2-methyl propane sulfonic acid (AMPS abbreviated as AP), and blended with cellulose acetate (CA) in dimethyl formamide. Scanning electron microscopy (SEM) showed much finer domain morphology for MA–PAN blends than AP–PAN blends. Dynamic mechanical property measurements showed an inward migration of the two glass transition temperatures (T_g) viz., T_g's of PAN and CA, however the migration of PAN T_g was more pronounced in AP–PAN blends, the result agreed well with the conjugate phase calculation. The phase inversion composition, calculated using Coran–Patel model agreed well with SEM morphology.

Keywords: Polyacrylonitrile; Cellulose acetate; Coran–Patel model

1. Introduction

Blending may be used effectively to modify the properties of polymer materials. This method is based on the theoretical possibility of controlling the properties of polymers by modifying their chemical compositions and molecular structures by means of the appropriate selection of miscible polymers [1–3]. Miscible polymer blends are really new materials with completely different properties, and fabricated articles may possess good mechanical properties. However, well established miscible polymer blends are very rare. Immiscible polymer blends generally have a coarse morphology which is reflected in their poor mechanical properties. If on the other hand it is possible to obtain a highly dispersed mixture from immiscible polymers, fabricated articles may combine the properties of the component polymers.

Polyacrylonitrile (PAN) and cellulose acetate (CA) have been the subject of current researches, because both polymers can easily produce fibers in a common organic solvent, e.g. *N*,*N*-dimethyl formamide (DMF). It has been reported [4–6] that PAN–CA blend is immiscible. However, if CA–PAN graft copolymer is added to this blend, considerable improvements in the homogeneity and the stability of the solution blends are obtained. Unfortunately, this system has not yet been industrialized due to the poor economic benefit of processing.

It has been known that PAN is rarely compatible with most other polymers due to the strong dipole–dipole interactions of nitrile groups [7,8]. However, CA is compatible with several synthetic polymers having electron-rich pendant group, such as poly(4-vinyl pyridine) [9,10]. Fiber-forming PAN has been generally modified with a small amount of amorphous vinyl monomers to give better processability and dyeability [11,12].

As a continuation of our earlier efforts to modify the properties of PAN [13–15], in this experiment we prepared two types of PAN copolymers with methyl acrylate (MA) and 2-acrylamido-2-methylpropane sulfonic acid (AMPS), and the miscibilities of these PAN copolymers with CA have been studied in terms of morphology, dynamic mechanical, and mechanical properties of the blends.

2. Experimental

2.1. Materials and preparation of samples

Cellulose acetate (CA) was purchased from Aldrich. The degree of polymerization and degree of substitution were 160 and 2.4, respectively. Copolymers containing 8 wt% of MA (hereafter called MA–PAN) and AMPS (hereafter called AP–PAN) were prepared as follows. Copolymerization was carried out in 50 wt% DMF at 70°C for 10 h under

* Corresponding author. Tel.: +82-51-510-2406; fax: +82-51-514-1726.
E-mail address: bkkim@hyowon.pusan.ac.kr (B.K. Kim)

0032-3861/00/$ - see front matter
PII: S0032-3861(99)00148-2

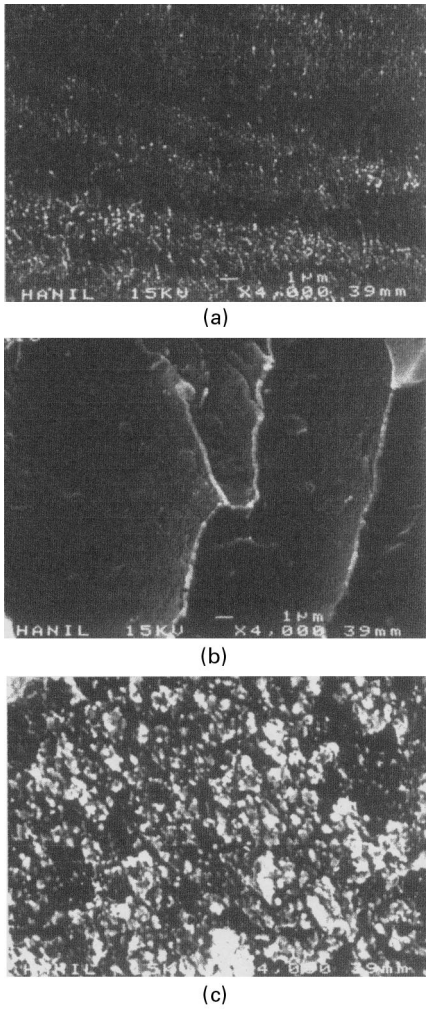

Fig. 1. SEM micrographs of the base polymers: (a) MA–PAN; (b) AP–PAN; and (c) CA.

nitrogen atmosphere. 0.4 wt% azobisisobutylonitrile (AIBN), based on the monomer weight, was used as a radical initiator. Upon completing the polymerization reaction, PAN solution was diluted in dimethyl formamide (DMF) and precipitated into water and washed three times with fresh water. The washed polymer was dried under vacuum at 50°C for 72 h.

The intrinsic viscosities $[\eta]$ of MA–PAN and AP–PAN were 1.24 and 1.31 dl/g in DMF at 35°C, respectively. PAN–CA solution blends of various compositions (80/20, 60/40, 40/60, and 20/80 by weight) were prepared by mixing the appropriate amounts of the component polymers in DMF for over 24 h at room temperature. Films were obtained by casting the solution on a glass plate, followed by drying under vacuum at 80°C for 72 h.

2.2. Tests

Morphologies were studied from the cryogenically fractured surface of the samples, sputtered with gold before viewing under a scanning electron microscopy (SEM, JSM 6400). Dynamic mechanical properties of the cast films were measured using a Rheovibron (Orientec DDV-01FP) at 11 Hz from 0 to 250°C with liquid nitrogen purging. Tensile properties at room temperature were measured following the standard procedure in ASTM D412 with type C specimen using a Tensilon (Shimudzu, Autograph S-100), operated at 50 mm/min. At least five runs were made to report the average.

3. Results and discussion

3.1. Morphology

Fig. 1 shows the SEM micrographs of CA, MA–PAN, and AP–PAN. A homogeneous morphology is observed with the modified PAN films (Fig. 1(a) and (b)), whereas aggregated particles are observed with CA film (Fig. 1(c)). The totally different morphologies are generated by the different driving temperatures for solidification. These films were cast at 70°C, which is close to the glass transition temperature (T_g) of PAN (about 80°C) and significantly lower than the T_g of CA (about 220°C). Therefore, aggregations into larger domains are possible for CA due to the great driving forces for solidifications.

SEM micrographs of the fractured surface for the MA–PAN–CA and AP–PAN–CA blends are shown in Figs. 2 and 3, respectively. Regardless of composition, AP–PAN–CA blends gave finer domain morphology compared to the MA–PAN–CA blends. In both types of blends, the domain size greatly increased from several micrometer to some tens of micrometer with increasing CA content. MA–PAN–CA blends have distinct boundaries between domains and matrix, implying poor interfacial adhesion. When CA is dispersed, the dispersed domains are elliptically deformed, implying that less viscous domains (CA) are sheared during the film casting step due to the evaporation of solvent. When PAN is dispersed, the domain is much smaller in AP–PAN–CA blends than in MA–PAN–CA blends.

The morphology of solvent cast film of polymer blend depends on a number of factors including the composition of the blend, the history of the solution, the rate of solvent evaporation, and solution viscosity. However, the size of the dispersed domains is largely governed by the level of polymer miscibility. The domain reduction and relatively good interfacial adhesion in AP–PAN–CA blends can be explained by the interactions between proton accepter, viz. the acetyl group in CA and proton donor, viz. sulfonic acid of the modifier unit in AP–PAN. In addition, higher capability of hydrogen bondings between acetyl oxygens in CA and amide hydrogens in AP–PAN may also enhance the interfacial adhesion in AP–PAN–CA blends.

3.2. Dynamic mechanical properties

The dynamic mechanical properties of MA–PAN blends

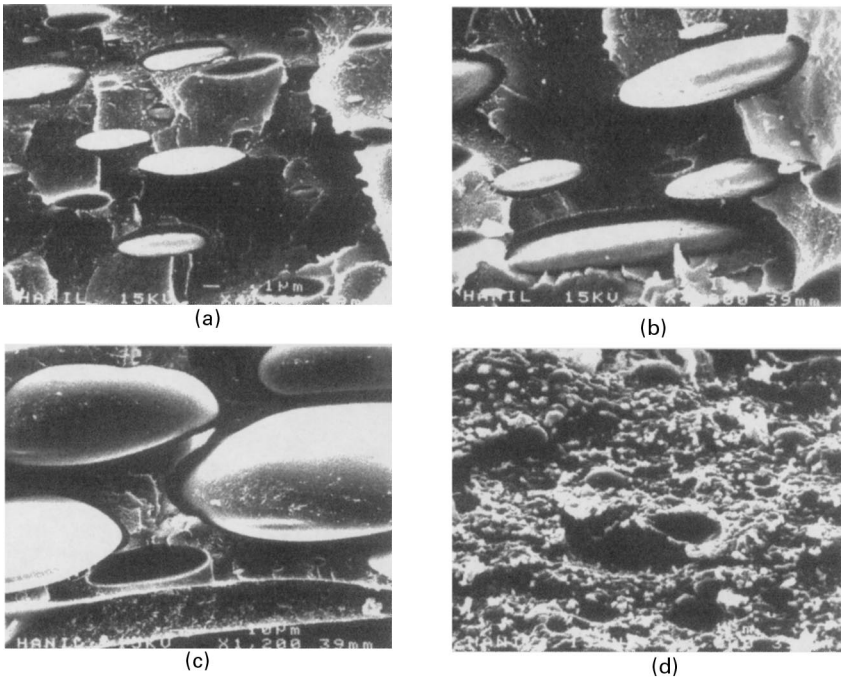

Fig. 2. SEM micrographs of MA–PAN–CA blends: (a) 80/20; (b) 60/40; (c) 40/60; and (d) 20/80.

are shown in Figs. 4 and 5 as a function of temperature. Virgin MA–PAN shows a large decrease in storage modulus around the T_g of approximately 70°C (see the loss tangent in Fig. 5). A further decrease in modulus above 200°C is associated with the thermal decomposition of this polymer. However, the modulus of virgin CA begins to drop off sharply at around its T_g, viz., 230°C. The tanδ peaks of their blends show two glass transitions. As CA is added, plateau modulus as well as the T_g of PAN increased, whereas the T_g of CA slightly decreased (Table 1).

The dynamic mechanical properties of AP–PAN–CA blends are shown in Figs. 6 and 7 as a function of temperature. The modulus and tanδ behavior of virgin AP–PAN is similar to that of virgin MA–PAN. As CA is added, the plateau modulus of AP–PAN monotonically increased in the PAN-rich blends implying the effective reinforcement

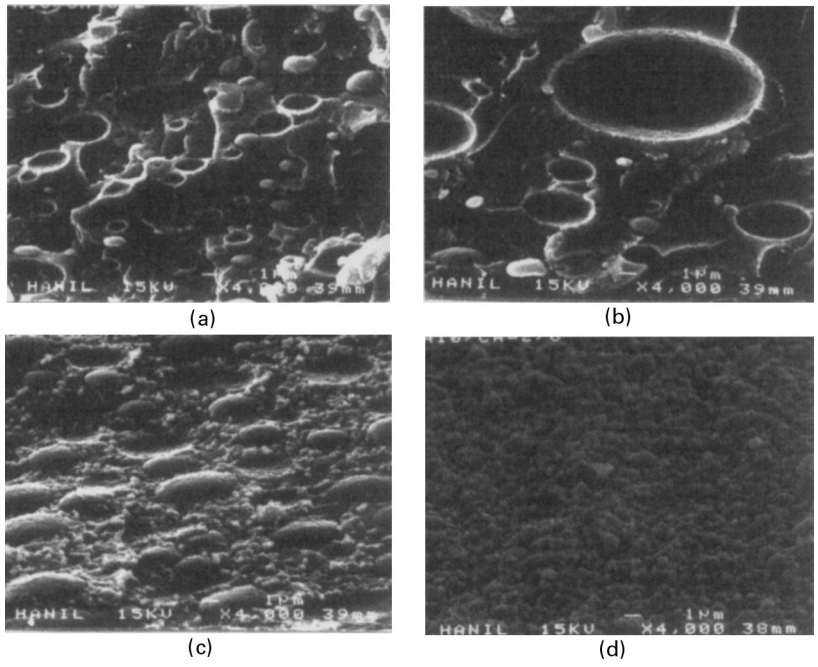

Fig. 3. SEM micrographs of AP–PAN–CA blends: (a) 80/20; (b) 60/40; (c) 40/60; and (d) 20/80.

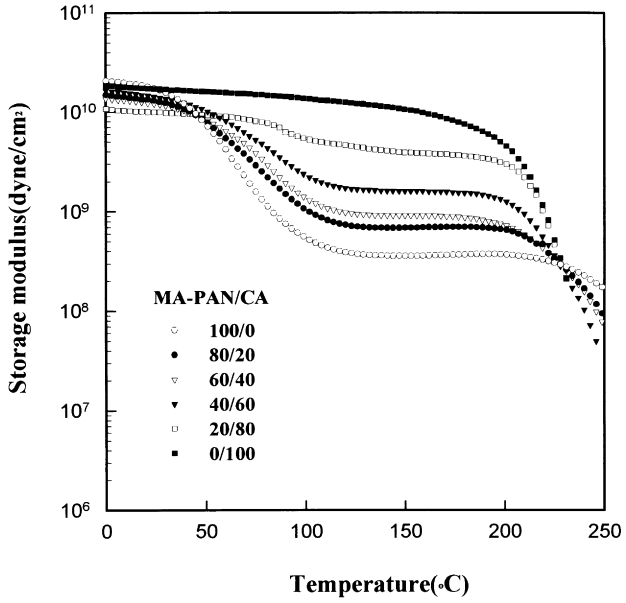

Fig. 4. Storage modulus vs. temperature for MA–PAN–CA blends.

of PAN matrix with CA particles. However, the plateau region of PAN disappeared in the CA-rich blends and a new transition region is observed. Blend T_g is given by [16].

$$\frac{1}{T_g} = \frac{W_1}{T_{g1}} + \frac{W_2}{T_{g2}}. \quad (1)$$

For conjugated phase [17,18],

$$W'_1 = \frac{T_{g2}(T_{g1} - T_{g1,b})}{T_{g1,b}(T_{g1} - T_{g2})} \quad (2)$$

$$W''_1 = \frac{T_{g1}(T_{g2,b} - T_{g2})}{T_{g2,b}(T_{g1} - T_{g2})} \quad (3)$$

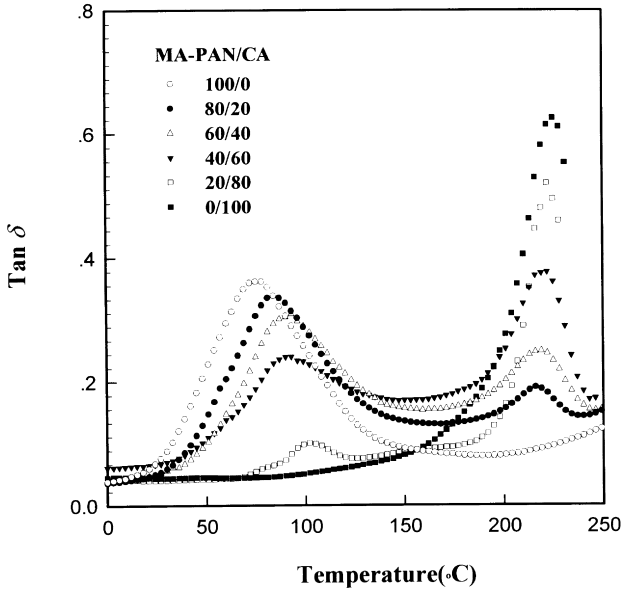

Fig. 5. Tanδ vs. temperature for MA–PAN–CA blends.

Table 1
Glass transition temperatures of blends obtained from tanδ peaks (°C)

CA content (wt%)	MA–PAN–CA blend		AP–PAN–CA blend	
	$T_{g,PAN}$	$T_{g,CA}$	$T_{g,PAN}$	$T_{g,CA}$
0	78	–	87	–
20	84	216	99	213
40	93	219	108	216
60	95	222	117	218
80	98	224	122	220
100	–	226	–	226

where, W_i is the weight fraction of component i in blend (1 and 2 designate PAN and CA, respectively), and W'_i, W''_i are the weights in PAN-rich and CA-rich phase, respectively. The compositions of the conjugated phases were calculated using the tanδ peaks as their glass transition temperature (Table 2). In both types of blend the solubility of CA in PAN is much greater than PAN in CA. And this tendency is more pronounced in AP–PAN–CA blends than in MA–PAN–CA blends.

3.3. Modulus behavior at 80°C

For a heterogeneous system, a broad range of modulus behavior is expected, depending on morphology, the degree of phase interpenetration, the size, and distribution of phase domains. A number of mechanical models are available for evaluating such features as phase continuity and phase inversion. For simplicity, the parallel arrangement of discrete phases provides as absolute upper limit on the dynamic mechanical modulus of the blend:

$$E_U = \phi_H E_H + \phi_S E_S \quad (4)$$

where, E_U is the blend modulus, E_H and E_S are moduli of the

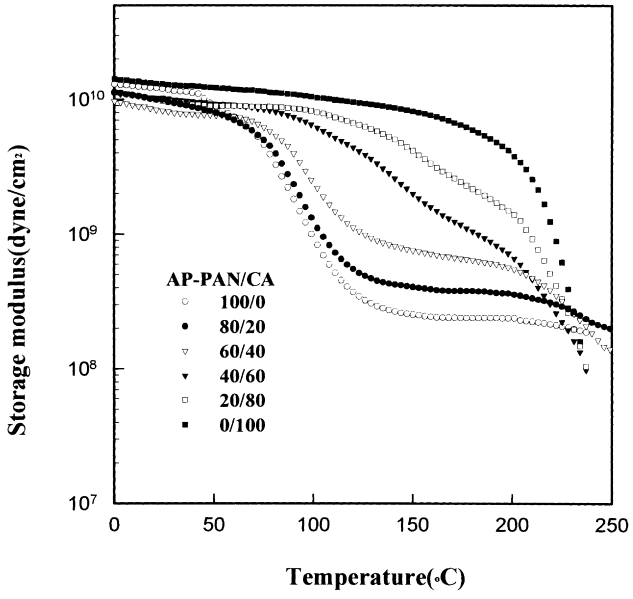

Fig. 6. Storage modulus vs. temperature for AP–PAN–CA blends.

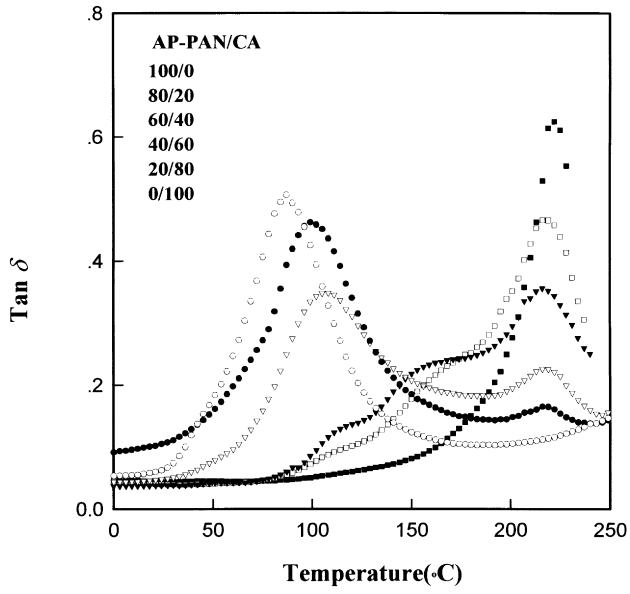

Fig. 7. Tanδ vs. temperature for AP–PAN–CA blends.

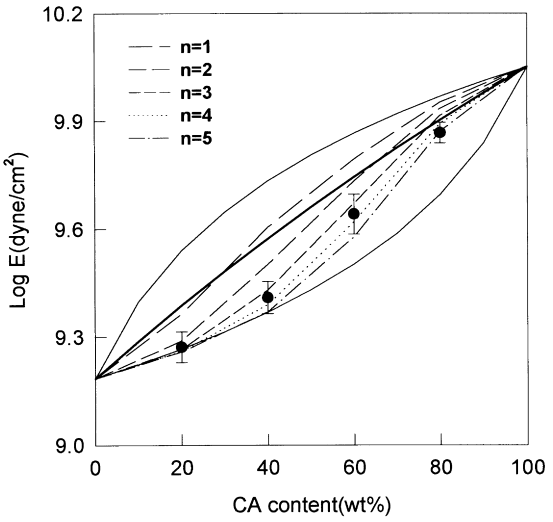

Fig. 8. Complex moduli of MA–PAN–CA blends at 80°C, and comparison with upper–lower bound model (solid line), Davis model (bold solid line), and Coran–Patel model (dashed line).

hard and soft phases; H and S are the volume fractions of the hard and soft phases, respectively. A series arrangement of discrete phases gives an absolute lower limit on the blend modulus

$$E_L = \left(\frac{\phi_H}{E_H} + \frac{\phi_L}{E_L} \right)^{-1}. \quad (5)$$

The upper–lower limit model (parallel–series model) defines the bounds on the modulus. These bounds are based on the assumption that properties of blend components are the same in the blend as in bulk. A dual phase continuity model proposed by Davies [19], which accounts for the phase interaction, is

$$E^{1/5} = \phi_1 E_1 + \phi_2 E_2^{1/5} \quad (6)$$

where, E is the blend modulus. E_i and ϕ_i are moduli and volume fractions of each component. And finally, the Coran–Patel model [20,21], which represents a phenomenological adjustment between the parallel and series models and characterized as a one-parameter model, is

$$E = \phi_H^n (n\phi_S + 1)(E_U - E_L) + E_L \quad (7)$$

where, E_U is the upper bound (Eq. (4)) and E_L is the lower bound (Eq. (5)) and n is an adjustable parameter related to the change in phase morphology as a function of H. The logarithmic complex moduli of MA–PAN–CA and AP–PAN–CA blends at 80°C are shown in Figs. 8 and 9, respectively. The solid lines represent upper and lower bounds that were calculated using the moduli of the two modified PAN and CA films. The bold solid line represents Eq. (6) viz., Davies model. Weight fractions were substituted for volume fraction in the equations. MA–PAN–CA blends (Fig. 8) show negative deviation from the Davies model, whereas AP–PAN–CA blends (Fig. 9) are relatively well fitted with the model. These results imply that interfacial interactions are poor in MA–PAN–CA blends and relatively good in AP–PAN–CA blends, and the results are consistent with

Table 2
Apparent weight fractions of conjugated phase of blends calculated from T_g data

CA content (wt%)	MA–PAN–CA blend		AP–PAN–CA blend	
	W''_1	W'_2	W''_1	W'_2
20	0.049	0.059	0.069	0.116
40	0.034	0.138	0.053	0.198
60	0.019	0.156	0.042	0.276
80	0.009	0.182	0.032	0.318

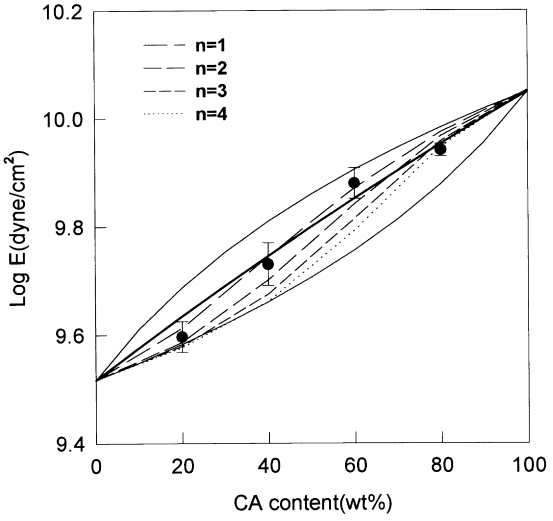

Fig. 9. Complex moduli of AP–PAN–CA blends at 80°C, and comparison with upper–lower bound model (solid line), Davis model (bold solid line), and Coran–Patel model (dashed line).

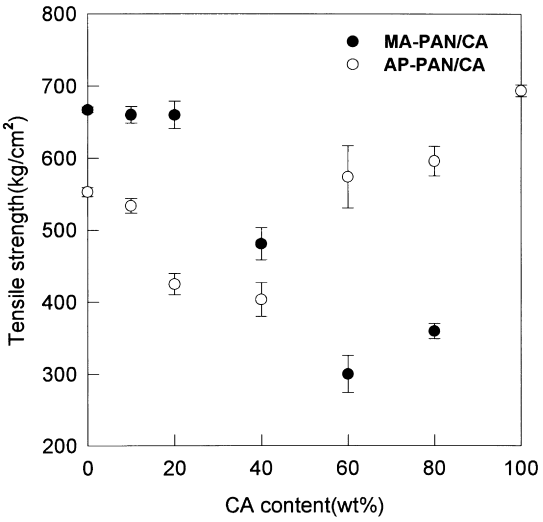

Fig. 10. Tensile strength of blends as a function of CA content.

dynamic mechanical data and morphology. For MA–PAN–CA blends, the 80/20 blend is fitted with $n = 3$ of the Coran–Patel model (Eq. (7)), 40/60 and 60/40 blends with $n = 3$–4, and the 20/80 blend with $n = 5$, and the experimental values are generally well fitted with $n = 3$–4. However, in the AP–PAN–CA blend, experimental values are well fitted with $n = 1$–2. $(n - 1)/n$ indicates the center of the H range where phase inversion or transition occurs. Thus, it can be noted that phase inversion takes place at $H = 0.67 - 0.75$ (MA–PAN–CA) and 0.5–0.67 (AP–PAN–CA blend). These results agree well with SEM morphologies (Fig. 1(c) and (d), Fig. 2(b) and (c)).

3.4. Tensile properties

The tensile strengths of the blends as a function of CA content are shown in Fig. 10. As a result of the immisciblity, both types of blend show negative deviation from the simple additivity. However, the negative deviation is much greater for MA–PAN–CA blends with a minimum at 60/40, as compared with AP–PAN–CA blends which show a minimum at 40/60 composition. These minimum compositions are related to the domain size, and indirectly indicate the compositions of maximum domain size of the dispersed CA phase.

4. Conclusions

MA and AP were respectively used as comonomers to modify PAN. Solution blends of the two types of modified PAN with CA showed partial miscibility, evidenced by the inward migration of the two T_g. The migration of T_g was much greater with PAN than with CA, indicative of greater solubility of CA in PAN, a result consistent with the conjugate phase calculations.

Among the two types of modifed PAN, the AP–PAN blends showed much finer domain morphology, greater inward migration of T_g, and were well fitted with the Davies model. All these indicate better miscibility and interfacial adhesions as well, which on the other hand, can be introduced by proton acceptor (acetyl group in CA)-proton donor (sulfonic acid modified unit in AP–PAN), and strong hydrogen bondings between the acetyl oxygen of CA and amide groups of the AP–PAN.

The SEM micrographs showed that phase inversion occurred at 60/40 for MA–PAN–CA, and 40/60 for AP–PA–CA blends, the compositions corresponding to the tensile strength minimum, and predicted by the Coran–Patel model.

References

[1] Smith WA, Barlow JW, Paul DR. J Appl Polym Sci 1981;26:4233.
[2] El-Begawy SEM, Huglin MB. Eur Polym J 1991;27:1023.
[3] Cesteros LC, Isasi JR, Katime I. J Polym Sci, Polym Phys 1994;32:223.
[4] Gujot A, Benevise JP. J Appl Polym Sci 1962;6:9.
[5] Naimark NI, Vasil′ev BV, Zaspinok GS, Lozhkim NY. Vysokomol Soyed 1970;A12:1641.
[6] Siahkolah MA, Walsh WK. Text Res J 1974;44:895.
[7] Kim BK, Oh YS, Lee YM. J Macromol Sci-Phys 1994;B33(2):243.
[8] Cates DM, White HJ. J Polym Sci 1956;20:181.
[9] Aptel P, Cabasso I. J Appl Polym Sci 1980;25:1969.
[10] Cabasso I. Coatings Plastics Chem Prepr 1980;5:359.
[11] Gupta AK, Songhal RP. J Polym Sci, Polym Phys Ed 1983;21:2243.
[12] Dalven PI, Hilderbandt JR, Laccetti AT, Hongins LT, Gregor HP. J Appl Polym Sci 1985;30:1113.
[13] Oh YS, Kim SR, Lee S, Kim BK. J Macromol Sci-Phys 1995;B34(3):199.
[14] Oh YS, Kim BK. J Macromol Sci-Phys 1997;B36(5):667.
[15] Oh YS, Kim BK. Polymer 1997;38(20):5211.
[16] Suess M, Kressler J, Kammer HW. Polymer 1987;28:957.
[17] Kim BK, Choi CH. Polymer 1996;37(5):807.
[18] Kolarik J, Lednicky F. Polym Engng Sci 1992;32:886.
[19] Allen G, Bowden MJ, Todd SM, Blundell DJ, Jeffs GM, Davis WEA. Polymer 1974;15:28.
[20] Coran AY, Patel RP. J Appl Polym Sci 1976;20:3005.
[21] Coran AY, Patel RP. Rubber ChemTechnol 1983;56:210.